

Analysis of Advanced Space Vector PWM Techniques Extended to Over-Modulation Region for Induction Machine Drive

by Sahu Mithun

Submission date: 24-Jul-2021 05:32PM (UTC+0530)

Submission ID: 1623432978

File name: main3.pdf (4.73M)

Word count: 3413

Character count: 17125

Analysis of Advanced Space Vector PWM Techniques Extended to Over-Modulation Region for Induction Machine Drive

¹ Sahu Mithun

School of Electrical Sciences

Indian Institute of Technology Bhubaneswar

Bhubaneswar, India

sm81@iitbbs.ac.in

Dipankar De

School of Electrical Sciences

Indian Institute of Technology Bhubaneswar

Bhubaneswar, India

dipankar@iitbbs.ac.in

Burle Tulasi Rao

School of Electrical Sciences

Indian Institute of Technology Bhubaneswar

Bhubaneswar, India

btr10@iitbbs.ac.in

Akshat Vijaywargiya

School of Electrical Sciences

IIT Bhubaneswar

Bhubaneswar, India

av25@iitbbs.ac.in

Niladri Bihari Puhon

School of Electrical Sciences

Indian Institute of Technology Bhubaneswar

Bhubaneswar, India

nbpuhan@iitbbs.ac.in

Abstract—This paper focuses on the extension and associated analysis of advanced Space Vector PWM techniques (SVPWM) reported in the literature to the over-modulation zone of operation. The over-modulation operation is separated into two zones in conventional manner namely, zone-I and zone-II. The combination of sequence 0121 (in under modulation zone) and 121 (in over modulation zone during switching interval only) to achieve reduction in high frequency flux ripple while the low frequency components due to over-modulation remains nearly unchanged. This method is compared with 012 (in under modulation zone) and 12 (in over modulation zone during switching interval only) sequence. In both the cases, a smooth transition between linear and over modulation zones can be achieved. The analysis is carried out for computing RMS stator flux ripple and the harmonic distortion factor at different frequency of operation. The theoretical observation are verified through simulation and experimental studies.

Index Terms—Space Vector PWM technique, Over-Modulation region, Stator flux ripple, Flux distortion factor

INTRODUCTION

The application of space vector PWM technique is well known [1]–[21] for three phase induction machine drives. A diagram of three phase IM drive is shown in Fig. 1 where the DC bus could be obtained from a rectifier or a front end converter. The space vector PWM is an alternative technique to sine-triangle PWM to get the switching pulses for the three phase inverter. There are total eight different combinations in which the inverter (2-level) switches can be made ON or OFF [10]–[8]. The zero vectors (V_0 , V_7 in Fig. 1) are obtained when all the upper or all the lower switches are made ON together (it is a free-wheeling state for the three phase current as well). On the other hand the active vectors (V_1 , V_3 , V_5 , V_7 , V_6 , V_4 , V_2 , V_1 in Fig. 1) are obtained when some poles of the inverter are connected with positive DC bus and rest of the poles are connected with negative DC bus. The active vectors

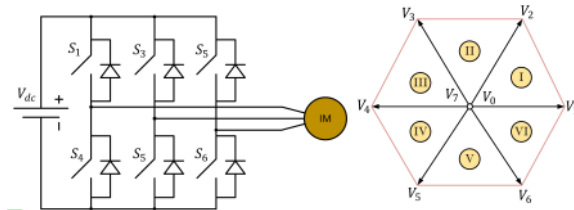


Fig. 1. Circuit Diagram of Three Phase VSI fed Induction Motor Drive and different available vectors from two level VSI

are usually normalized by V_{dc} (DC bus voltage) and displaced by 60° in space vector plane. The space vector technique utilizes 15% additional DC bus voltage (it can also be achieved by sine PWM technique when a third harmonic components is added with the reference sine waveform) and as the three phase available vectors are selected in a particular manner to synthesize a rotating vector, SVPWM method provides a direct control over the associated deviation in flux, torque from the steady state value due to PWM switching pattern. The zero vectors, in conventional space vector PWM techniques, are divided in equal halves. In Bus-Clamping space vector PWM technique, the zero vector is continuously applied for its specified time. The active vectors are distributed in two equal halves at different timings in a sampling period in case of Advanced Bus-Clamping Space Vector PWM technique. In sequences like 012, 120, 721 and 217 (which is also known as continually clamped SVPWM techniques), the zero vector applied once. On the other hand, sequences like 0121, 1210, 7212, and 2127 (advanced bus-clamping sequence) have one of the active vectors equally divided in the sampling time. These modified PWM sequences are mainly applied to achieve

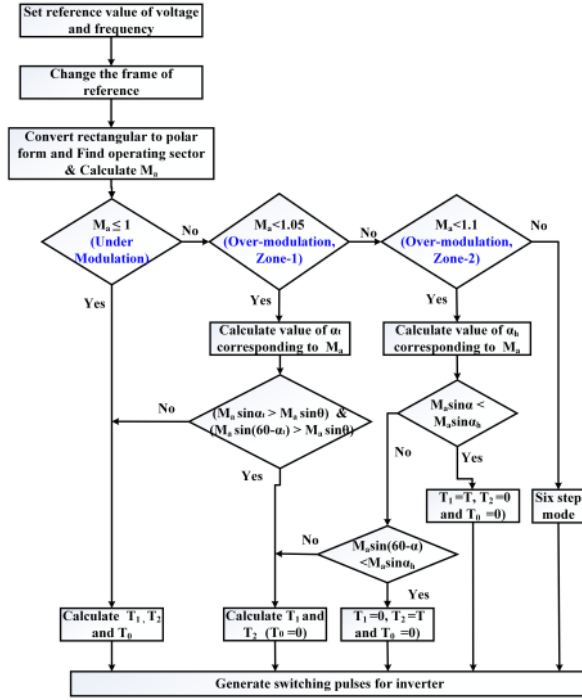


Fig. 2. Flow Chart for Implementing Space Vector PWM extended to over modulation zones [17]

either reduced switching frequency operation or reduced flux or torque ripple [9]–[12]. This ripple gets enhanced when the drive operates in the over-modulation zone in order to extract additional DC bus utilization at the cost of increased harmonics in the machine. The PWM techniques are applied to over-modulation zone in order to maintain the extended linearity beyond the unity modulation index [13]–[17]. In this work, the sequences with 0121 and 012 are extended to the over modulation zone to achieve the reduction in high frequency flux ripple while low frequency components due to over-modulation remains the same. A detailed relative comparisons are carried out both in linear modulation and over modulation zones. However, the effectiveness decreases as the operation reaches towards six-step mode. A detailed simulation results/analysis are presented.

This paper is organized as follows. Section II explains about the implementation technique of the proposed SVPWM technique with extended operation in over modulation zone. Section III gives the details about the stator flux ripple over a sub-cycle and associated calculation in over-modulation zone. The section IV provides the simulation and experimental verification results. Section V explains the conclusion of the work.

II. IMPLEMENTATION OF THE SVPWM TECHNIQUES

The flow chart for implementation of space vector PWM is shown in Fig. 2. For implementation of space vector PWM

technique both in linear modulation and over modulation zones, the following steps should be followed:

Step-1: Based on the desired operating point the voltage and frequency reference are set.

Step-2: The next step is to convert the three phase voltages using $abc-\alpha\beta$ conversion. The relationship between three phase voltage V_a, V_b, V_c and the converted voltages in $\alpha-\beta$ domain V_α and V_β can be written as

$$V_\alpha = \frac{2}{3} \left[V_a - \frac{V_b}{2} - \frac{V_c}{2} \right] = V_a \quad (1)$$

$$V_\beta = \frac{2}{3} \left[\frac{\sqrt{3}}{2} V_b - \frac{\sqrt{3}}{2} V_c \right] = \frac{1}{\sqrt{3}} [V_b - V_c] \quad (2)$$

Step-3: The next step is to convert V_α and V_β into its polar form (angle and magnitude). The modulation index, M_a can easily be evaluated from the magnitude.

Step-4: In this step the operating sector is identified from the angle of the vector and the suitable vectors to be applied are selected. The timings for these selected vectors are then evaluated based on its zone of operation as indicated in the next step.

Step-5: In this step, the suitable operating zone is identified using the value of modulation index M_a . It can be noted that this operating zone indicates whether the system operates in under modulation, over-modulation zone-I or over modulation zone-II or in six step mode [17].

- 1) If $M_a < 1 \Rightarrow$ under-modulation zone or linear modulation zone
- 2) If $1 < M_a < 1.05 \Rightarrow$ over-modulation zone-I
- 3) If $1.05 < M_a < 1.1 \Rightarrow$ over-modulation zone-II
- 4) If $M_a > 1.1 \Rightarrow$ six-step mode

The timing computation for vector in different zones are explained below.

In linear-modulation region, for example, if the reference vector lies in sector-1, V_1 is applied for T_1 s, V_2 is applied for T_2 s and zero vector is applied for T_0 s. These timings can be written as [5]

$$T_1 = V_{Ref} \frac{\sin(45^\circ - \alpha)}{\sin(60^\circ)} T \quad (3)$$

$$T_2 = V_{Ref} \frac{\sin(\alpha)}{\sin(60^\circ)} T \quad (4)$$

$$T_0 = T - T_1 - T_2 \quad (5)$$

In over-modulation region zone-1, firstly, the value of the angle is evaluated according to M_a . When the reference vector lies inside the hexagon (or more precisely within an angle α_t from the starting and from the end of the sector [17]), the timings are computed exactly like the under-modulation region (Fig. 2). If the reference vector lies outside the above region, only active vectors are operated (as shown in Fig. 3), the time

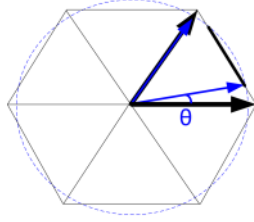


Fig. 3. Illustration of operation in Zone-I (over modulation)

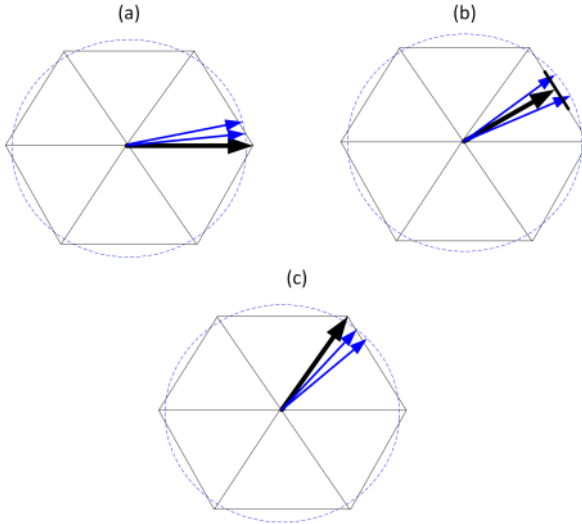


Fig. 4. Illustration of operation in Zone-II (over modulation)

for zero vector becomes zero. During this operating mode the effective applied vector in a switching interval travels along the hexagon boundary. If V_1 is applied for T_1 s, V_2 is applied for T_2 s, they can be related as

$$T_1 = \frac{\sin(60^\circ - \alpha)}{\sin\alpha + \sin(60^\circ - \alpha)} T \quad (6)$$

$$T_2 = T - T_1 \quad (7)$$

In over modulation zone-2 (as shown in Fig. 4), the first the value of α_h is calculated according to M_a [17]. When the reference vector lies within an angle α_h from the stator and from the end of the sector, the nearest active vector is applied continuously [in Fig. 4 (a) and (c)]. For the other values of angles, the converter switches like zone-1 [with the timings given in (6) and (7)]. These steps are summarized in Fig. 2.

Step-6: Once the timings are determined indicated above the reference signal is generated. This reference signal then compared with a carrier signal of suitable frequency to generate the gating pulses for the inverter.

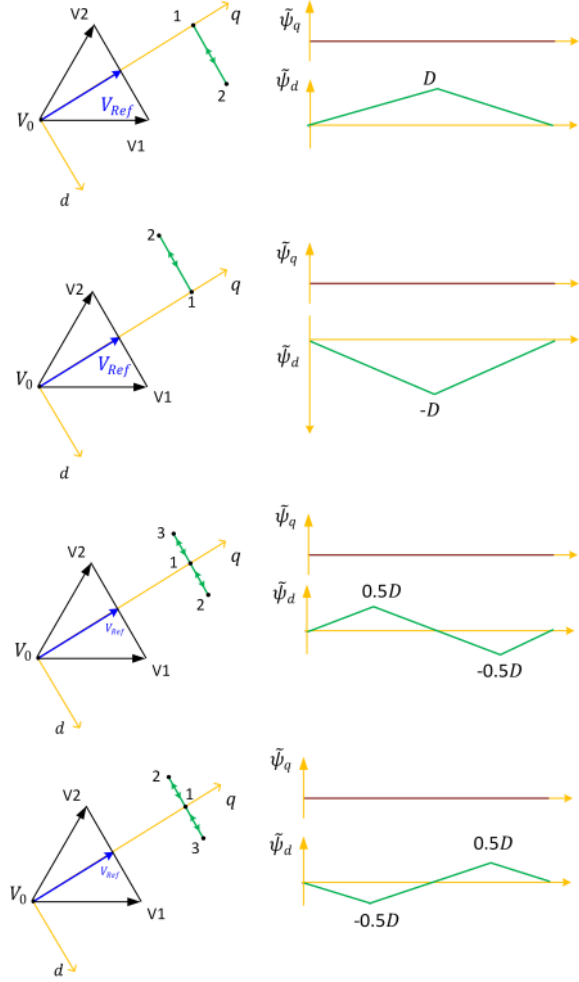


Fig. 5. Stator flux ripple with d-q components during over modulation (for a particular position of the vector at the centre of sector-1 ignoring any low frequency harmonics in the flux (a general case is shown in Fig. 6

III. STATOR FLUX RIPPLE OVER A SUB-CYCLE IN OVER MODULATION REGION

When the tip of the applied vector (synthesized) is on the boundary of the hexagon, only the active vectors are required to be applied. Let us first consider a simplified situation where the synthesized vector is exactly at the centre of the hexagon as shown in Fig. 5. Further, it is assumed that there is no low frequency harmonics due to over modulation (due to over modulation operation there will certainly be harmonics and this will be discussed in the next paragraph). It can be observed from Fig. 5, the flux error vector has zero q-axis component and a d-axis component is present in this particular case. The stator flux ripple vector and its d-axis and q-axis components are shown in Fig. 5. Fig. 5 (1st figure

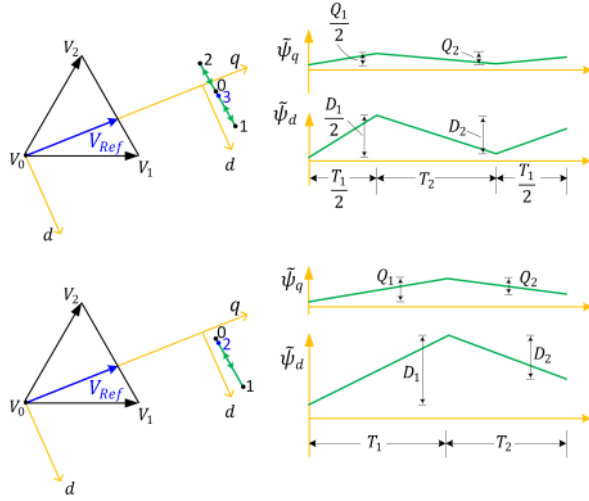


Fig. 6. Stator flux ripple with d-q components during over modulation (for a general of the vector considering low frequency harmonics in the flux due to over modulation)

from the top) shows the swing of flux error vector due to one possible combination of the applied voltage vectors. When V_1 is applied the operating point moves from '1' to '2' and corresponding d-axis error flux increases linearly from 0 to its maximum value. When V_2 is applied, the operating point moves back to point-1 again. In the second figure in Fig. 5, V_2 applied before V_1 and the associated movement in the operating point is in the negative direction of d-axis. The square of the RMS values of q- and d- axis flux error in these two cases (above) can be written as respectively:

$$\Psi_q^2 = 0 \quad (8)$$

$$\Psi_d^2 = \frac{1}{3} D^2 \frac{(T_1 + T_2)}{T} \quad (9)$$

When the vector (synthesized) in the over modulation zone is on the hexagon boundary, the vectors required to be applied are active vectors only. Hence,

$$T_1 + T_2 = T \quad (10)$$

Hence (9) can be written as,

$$\Psi_d^2 = \frac{1}{3} D^2 \quad (11)$$

The RMS value of stator flux ripple over a sub-cycle for reference vector can be written as

$$F^2 = \Psi_q^2 + \Psi_d^2 = \frac{1}{3} D^2 \quad (12)$$

The third possible combination of the applied vector (121) in the over modulation zone as shown in Fig. 5 forces the operating point movement as follows:

- 1) $1 \rightarrow 2$ when V_1 is applied for $T_1/2$
- 2) $2 \rightarrow 3$ when V_2 is applied for T_2

- 3) $3 \rightarrow 1$ when V_1 is applied for $T_1/2$

In this case time T_1 is divided equally in two halves. Similarly, the division of T_2 in two equal halves are shown in Fig. 5 (the last or 4th figure).

- 1) $1 \rightarrow 2$ when V_2 is applied for $T_2/2$
- 2) $2 \rightarrow 3$ when V_1 is applied for T_1
- 3) $3 \rightarrow 1$ when V_2 is applied for $T_2/2$

In the third or fourth case, d-axis component of the error flux is given by

$$\Psi_d^2 = \frac{1}{3} 0.5 D^2 \frac{(T_1 + T_2)}{T} = \frac{1}{3} 0.5 D^2 \quad (13)$$

As the q-axis component of the error flux is zero in this case, the RMS value of stator flux ripple over a sub-cycle for reference vector on hexagon is given as

$$F^2 = \Psi_q^2 + \Psi_d^2 = \frac{1}{3} (0.5 D)^2 \quad (14)$$

However, the results obtained above considers the case where the synthesized vector lies in the middle of the hexagon and when there is no low frequency harmonics are present. A more generalized and practical scenario is presented in Fig. 6. It can be observed that the q-axis components will not be zero if the vector location is slightly different from the centre of the hexagon. Moreover, it will have a initial condition at the beginning of the switching period in both d and q axis flux error components. At the end of that particular switching interval the component does not come to the same initial value. Fig. 6 shows d- and q- axis error flux respectively for 0121 (121 in over modulation zone non-clamped portion) and 012 (12 in over modulation zone non-clamped portion). The RMS values of the error flux vector can be obtained for 012 as in (15) and (16). In these equations, D_1 , Q_1 , D_2 , Q_2 are indicated in Fig. 6 and ΔD and ΔQ are the initial conditions for the d and q axis respectively at the beginning of the switching period. Please note that at the end of the switching period the values of ΔD_{new} and ΔQ_{new} are given as $\Delta D + D_1 - D_2$ and $\Delta Q + Q_1 - Q_2$ respectively. The Fig. 7 shows the RMS Stator Flux Ripple for Modulation index of 0.9, 1.02, 1.06, 1.09 for 012 and 0121 sequences for different angles at sector-1. It can be observed that at over-modulation region flux ripple is high compared to that in under modulation region. In under modulation zone 0121 provides a better performance. The Fig. 8 shows the total RMS Harmonic Distortion Factor with frequency variations for different sequences. The results are provided for both linear and over modulation region. In over-modulation region, the 012 sequence and 12 sequence provide nearly similar results.

IV. SIMULATION AND HARDWARE RESULTS

The simulation results are shown in Fig. 9 for different values of modulation index. The simulations are carried out in PLECS software. In this figure, the simulation results (R-phase voltage, R-phase current and sector) due to sequence 0121 in linear modulation + 121 in over modulation at different voltage reference voltages are shown. In order to confirm the analysis

$$\Psi_d^2 = \frac{1}{T} [(D_1 + \Delta D)^2 T_2 + (\Delta D)^2 T_1 + \Delta D D_1 T_1 - D_2 (D_1 + \Delta D) T_2 + D_1^2 T_1/3 + D_2^2 T_2/3] \quad (15)$$

$$\Psi_q^2 = \frac{1}{T} [(Q_1 + \Delta Q)^2 T_2 + (\Delta Q)^2 T_1 + \Delta Q Q_1 T_1 - Q_2 (Q_1 + \Delta Q) T_2 + Q_1^2 T_1/3 + Q_2^2 T_2/3] \quad (16)$$

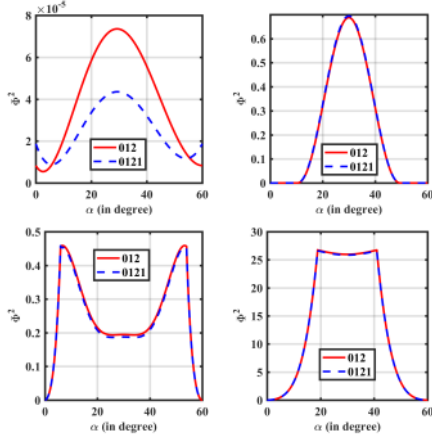


Fig. 7. RMS Stator Flux Ripple for Modulation index of 0.9, 1.02, 1.06, 1.09 respectively

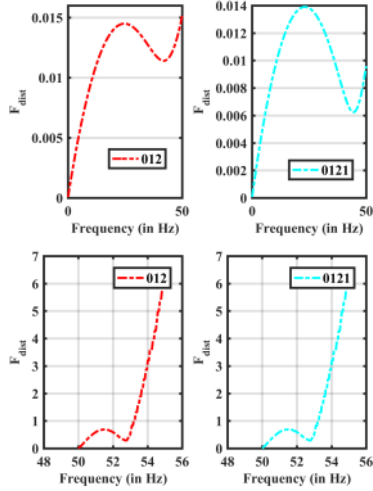
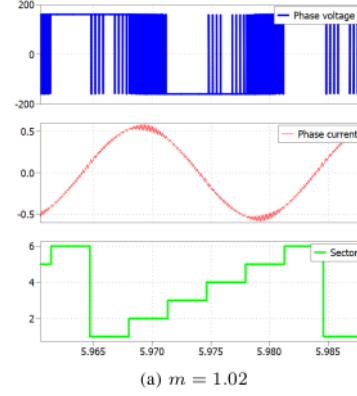
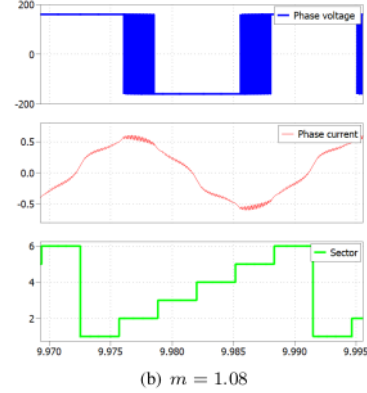


Fig. 8. Total RMS Harmonic Distortion Factor with frequency variation: (above) Under modulation zone, (below) Over modulation zone

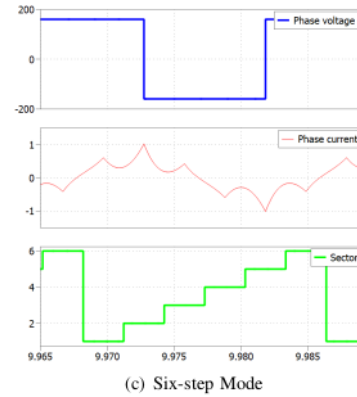
and simulation studies, a reduced rating hardware prototype is built. The Fig. 10(a) shows the hardware set up for the experimental verification. The set-up consists of an induction motor fed by three phase inverter. For providing the DC bus voltage, a three phase diode bridge rectifier is used. The rectifier is energised through a three phase auto transformer. An inductor is utilized as filter for rectifier output. For the inverter switches, switching pulses are required. For generating



(a) $m = 1.02$



(b) $m = 1.08$



(c) Six-step Mode

Fig. 9. Simulation Results in PLECS: The voltage between inverter phase to DC bus neutral, phase current and operating sector for 0121 sequences in Over-modulation region at different voltage references

switching pulses, a digital signal processor TMS320F28335 is used. The DSP board generate 6 PWM signals which are combined with XOR gate to regenerate 3 desired PWM signals for the inverter. These signals are given to protection and delay card to 6 signals for six switches including the effect of dead-time. The values of α_h and α_t for over-modulation zone-II and zone-I respectively are stored as look-up table in digital signal processor memory for different modulation index values from linear modulation to over modulation zone.

For 0121 sequences, the Fig. 10 shows experimentally measured R-phase pole voltage, line current (R-phase) and sector information at different modulation index values in 10(b) to 10(f).

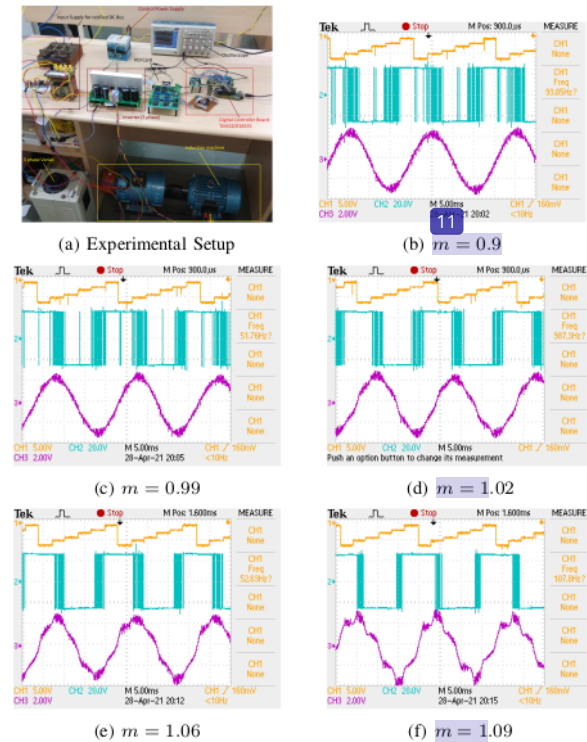


Fig. 10. Measured Experimental results for different modulation index: Ch1: sector information, Ch2: Phase voltage (R-phase) (200V/div), Ch3: Line current (R-phase) (2 A/div)

V. CONCLUSION

The voltage source inverters fed AC drives operate in over-modulation zone for higher DC bus utilization and for extended linear operation. The paper proposes a scheme to operate the system in over-modulation zone-I and over modulation zone-II are presented for the extended operation of the advanced PWM sequences. The analysis shows that 0121 (in under modulation zone) + 121 (in over modulation zone) provides better performance in under modulation zone and in selected range in over modulation zone compared

to its continually clamped version. An comparative study between the sequence 0121 and 012 in the extended over-modulation zone are presented. The performance of the system is analysed with error-flux RMS value computation in d and q axis over a sector for different modulation index values (upto six step mode) and frequency dependent distortion factor are evaluated. The concept is verified through detailed simulation and experimental studies. The study and analysis can easily be extended to any other SVPWM sequences as well.

REFERENCES

- [1] D. G. Holmes and T. A. Lipo, "Pulse Width Modulation for Power Converters: Principle and Practice". New York: Wiley, 2003.
- [2] K. Zhou and D. Wang, "Relationship Between Space-Vector Modulation and Three-Phase Carrier-Based PWM: A Comprehensive Analysis", *IEEE Trans. Industrial Electron.*, vol. 49, no. 1, February 2002.
- [3] V. G. Agelidis, A. Balouktsis, I. Balouktsis, and C. Cossar, "Multiple sets of solutions for harmonic elimination PWM bipolar waveforms: Analysis and experimental verification," *IEEE Trans. Power Electron.*, vol. 21, no. 2, pp. 415-421, Mar. 2006.
- [4] A. M. Hava, R. J. Kerkman, and T. A. Lipo, "Simple analytical and graphical methods for carrier-based PWM-VSI drives", *IEEE Trans. Power Electron.*, vol. 14, no. 1, pp.
- [5] G. Narayanan, D. Zhao, H. K. Krishnamurthy, R. Ayyanar, and V. T. Ranganathan, "Space Vector Based Hybrid PWM Techniques for Reduced Current Ripple", *IEEE Trans. Industrial Electron.*, vol. 55, no. 4, April 2008.
- [6] K. Basu, J. S. Siva Prasad, and G. Narayanan, "Minimization of Torque Ripple in PWM AC Drives", *IEEE Trans. Industrial Electron.*, vol. 56, no. 2, Feb 2009.
- [7] T. Bhavsar and G. Narayanan, "Harmonic Analysis of Advanced Bus-Clamping PWM Techniques", *IEEE Trans. Power Electron.*, vol. 24, no. 10, Oct 2009.
- [8] S. R. Bowes and D. Holliday, "Optimal regular sampled PWM inverter control techniques," *IEEE Trans. Ind. Electron.*, vol. 54, no. 3, pp. 1547-1559, Jun. 2007.
- [9] G. Narayanan, and V. T. Ranganathan, "Analytical Evaluation of Harmonic Distortion in PWM AC Drives Using the Notion of Stator Flux Ripple", *IEEE Trans. Power Electron.*, vol. 20, no. 2, March 2005.
- [10] G. Narayanan, H. K. Krishnamurthy, D. Zhao, and R. Ayyanar, "Advanced Bus-Clamping PWM Techniques Based on Space Vector Approach", *IEEE Trans. Power Electron.*, vol. 21, no. 4, July 2006.
- [11] G. Narayanan and V. T. Ranganathan, "Analytical evaluation of harmonic distortion in PWM AC drives using the notion of stator flux ripple," *IEEE Trans. Power Electron.*, vol. 20, no. 2, pp. 466-474, Mar. 2005.
- [12] A. Cataliotti, F. Genduso, A. Raciti, and G. R. Gullazzo, "Generalized PWM-VSI control algorithm based on a universal duty-cycle expression: Theoretical analysis, simulation results, and experimental validations," *IEEE Trans. Ind. Electron.*, vol. 54, no. 3, pp. 1569-1580, Jun. 2007.
- [13] V. Kaura, and V. Blasko, "A Method to Improve Linearity of a Sinusoidal PWM in the Over-modulation Region", in *Proc. IEEE PEDES*, 2002, 33, (5), pp. 1254-1259.
- [14] V. Kaura, "A new method to linearise any triangle-comparison based PWM by reshaping the modulation command", *IEEE Trans. Ind. Appl.*, 1997, 33, (5), pp. 1254-1259.
- [15] G. Narayanan and V. T. Ranganathan, "Overmodulation algorithm for space vector modulated inverters and its application to low switching frequency PWM techniques", *IEE Proc.-Electr. Power Appl.*, Vol. 148, No. 6, November 2001.
- [16] Z. Peroutka, T. Glasberger, "Algorithms of space vector PWM in over-modulation area" *Advances in Electrical and Electronic Engineering*, 2011.
- [17] Alireza R. Bakhshai, Géza Joós, Praveen K. Jain, and Hua Jin, "Incorporating the Over-modulation Range in Space Vector Pattern Generators Using a Classification Algorithm", *IEEE Trans. Power Electron.* Vol. 15, No. 1, Jan. 2000.

Analysis of Advanced Space Vector PWM Techniques Extended to Over-Modulation Region for Induction Machine Drive

ORIGINALITY REPORT

17%

SIMILARITY INDEX

11%

INTERNET SOURCES

13%

PUBLICATIONS

2%

STUDENT PAPERS

PRIMARY SOURCES

- | | | |
|---|---|--|
| <div style="background-color: red; color: white; width: 40px; height: 40px; display: flex; align-items: center; justify-content: center; margin: 5px;">1</div> | <p>Srija Mukherjee, Abinash Dash, Dipankar De, Alberto Castellazzi. "Study of Dual Active Bridge with Modified Modulation Techniques for Harmonic Reduction in AC Link Current", 2019 IEEE International Conference on Sustainable Energy Technologies (ICSET), 2019</p> <p>Publication</p> | <div style="font-size: 2em; font-weight: bold;">2%</div> |
| <hr/> | | |
| <div style="background-color: purple; color: white; width: 40px; height: 40px; display: flex; align-items: center; justify-content: center; margin: 5px;">2</div> | <p>Ali Sarajian, Cristian Garcia, Quanxue Guan, Patrick Wheeler et al. "Over-modulation Methods for Modulated Model Predictive Control and Space Vector Modulation", IEEE Transactions on Power Electronics, 2020</p> <p>Publication</p> | <div style="font-size: 2em; font-weight: bold;">2%</div> |
| <hr/> | | |
| <div style="background-color: purple; color: white; width: 40px; height: 40px; display: flex; align-items: center; justify-content: center; margin: 5px;">3</div> | <p>www.coursehero.com</p> <p>Internet Source</p> | <div style="font-size: 2em; font-weight: bold;">1%</div> |
| <hr/> | | |
| <div style="background-color: teal; color: white; width: 40px; height: 40px; display: flex; align-items: center; justify-content: center; margin: 5px;">4</div> | <p>www.slideshare.net</p> <p>Internet Source</p> | <div style="font-size: 2em; font-weight: bold;">1%</div> |
| <hr/> | | |
| <div style="background-color: green; color: white; width: 40px; height: 40px; display: flex; align-items: center; justify-content: center; margin: 5px;">5</div> | <p>id.scribd.com</p> <p>Internet Source</p> | <div style="font-size: 2em; font-weight: bold;">1%</div> |
-

6

jpels.org
Internet Source

1 %

7

Rohit Goyal, B. Hemanth Kumar, Makarand M. Lokhande. "Combination of switching sequences in SVPWM to reduce line current ripple for IM drives", 2017 6th International Conference on Computer Applications In Electrical Engineering-Recent Advances (CERA), 2017

Publication

1 %

8

Ravi Teja Arumalla, Sheron Figarado, Nagendrappa Harischandrappa. "Analysis and Experimental Investigation of Double Switching Active Vector Sequences in Dodecagonal Space Vector Structure", IECON 2020 The 46th Annual Conference of the IEEE Industrial Electronics Society, 2020

Publication

1 %

9

M. R. Pooja Krishna, Ravi Teja Arumalla, Sheron Figarado, Krishnan Chemmangat. "Harmonic and switching loss analysis of two-level space vector based pulse width modulation schemes", IECON 2017 - 43rd Annual Conference of the IEEE Industrial Electronics Society, 2017

Publication

1 %

10

moam.info
Internet Source

1 %

11	vbn.aau.dk Internet Source	1 %
12	www.ijert.org Internet Source	1 %
13	Akagi. "The Instantaneous Power Theory", Instantaneous Power Theory and Applications to Power Conditioning, 02/02/2007 Publication	<1 %
14	R. Ayyanar. "Space Vector PWM with DC Link Voltage Control and Using Sequences with Active State Division", 2006 IEEE International Symposium on Industrial Electronics, 07/2006 Publication	<1 %
15	www.letag.com Internet Source	<1 %
16	Deliang Wu, Hafsa Qamar, Haleema Qamar, Raja Ayyanar. "Comprehensive Analysis and Experimental Validation of a New 240°- Clamped Space Vector PWM Technique Eliminating Zero States for EV Traction Inverters with Dynamic DC Link", IEEE Transactions on Power Electronics, 2020 Publication	<1 %
17	etd.ncsi.iisc.ernet.in Internet Source	<1 %

18

A.R. Bakhshai, G. Joos, P.K. Jain, Hua Jin.
"Incorporating the overmodulation range in
space vector pattern generators using a
classification algorithm", IEEE Transactions on
Power Electronics, 2000

Publication

19

Haw, Law Kah, Mohamed S. A. Dahidah, and
Haider A. F. Almurib. "SHE-PWM Cascaded
Multilevel Inverter With Adjustable DC Voltage
Levels Control for STATCOM Applications",
IEEE Transactions on Power Electronics, 2014.

Publication

20

R. Grinberg, P.R. Palmer. "Advanced DC Link
Capacitor Technology Application for a Stiff
Voltage-Source Inverter", 2005 IEEE Vehicle
Power and Propulsion Conference, 2005

Publication

21

Yifan Zhao, T.A. Lipo. "Space vector PWM
control of dual three-phase induction machine
using vector space decomposition", IEEE
Transactions on Industry Applications, 1995

Publication

22

Bhavani, J., J. Amarnath, and D. Subba
Rayudu. "Generalized PWM algorithm for VSI
fed induction motor drives using the only
sampled reference phase voltages", 2012 IEEE
5th India International Conference on Power
Electronics (IICPE), 2012.

<1 %

<1 %

<1 %

<1 %

<1 %

23

Olorunfemi Ojo. "A generalized over-modulation methodology for current regulated three-phase voltage source converters", Conference Record of the 2004 IEEE Industry Applications Conference 2004 39th IAS Annual Meeting, 2004

Publication

<1 %

24

W. Shireen, M.S. Arefeen, D. Figoli. "Controlling multiple motors utilizing a single DSP controller", IEEE Transactions on Power Electronics, 2003

Publication

<1 %

25

eprints.library.iisc.ernet.in
Internet Source

<1 %

26

hdl.handle.net
Internet Source

<1 %

27

idus.us.es
Internet Source

<1 %

28

"Handbook of Distributed Generation", Springer Science and Business Media LLC, 2017

Publication

<1 %

29

Narayanan, Gopalaratnam, Soumitra Das, and Arathil Chellappan Binojkumar. "Analytical evaluation of harmonic distortion factor corresponding to generalised advanced bus-

<1 %

clamping pulse width modulation", IET Power Electronics, 2014.

Publication

30

Joseph Peter, Rijil Ramchand. "Nearly constant switching frequency hysteresis controller for VSI fed IM drives based on Current Error Space Vector", 2016 IEEE International Conference on Power Electronics, Drives and Energy Systems (PEDES), 2016

Publication

<1 %

31

L. Helle, K.B. Larsen, A.H. Jorgensen, S. Munk-Nielsen, F. Blaabjerg. "Evaluation of Modulation Schemes for Three-Phase to Three-Phase Matrix Converters", IEEE Transactions on Industrial Electronics, 2004

Publication

<1 %

Exclude quotes On

Exclude matches < 4 words

Exclude bibliography On